

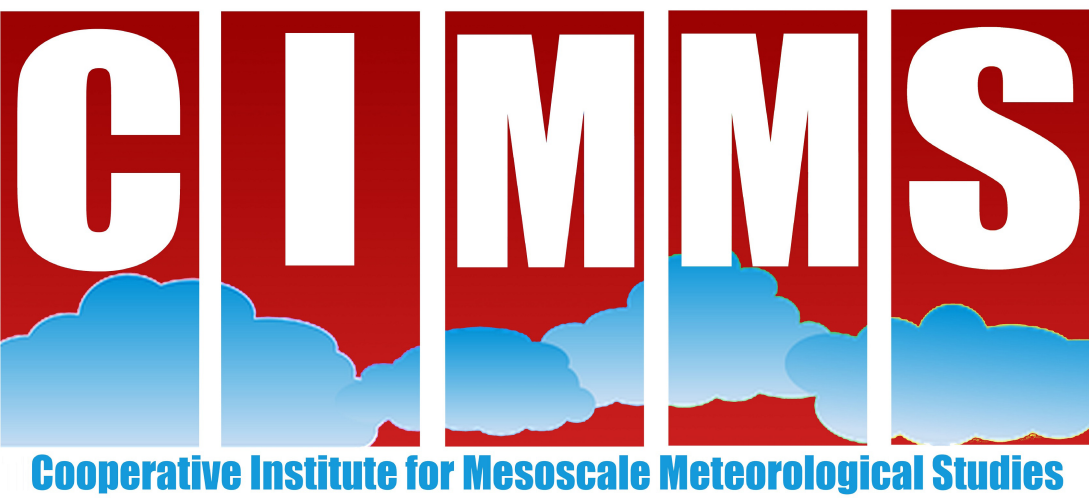
# Intercomparison Between Polarimetric Radar and Satellite Indicators of Storm Severity in a Tornadic Supercell

Michael M. French\* and Jeffrey C. Snyder+^

\*Stony Brook University, Stony Brook, NY

+CIMMS/Univ. of Oklahoma, Norman, OK

^NOAA/OAR/National Severe Storms Laboratory, Norman, OK



## Motivation

The upgrade of the WSR-88D network to dual-polarization capabilities and the upcoming launch of GOES-R have introduced potentially powerful new tools that can be used to learn more about storm severity. Specifically, enhanced values of differential radar reflectivity factor ( $Z_{DR}$ ) above the freezing level ( $Z_{DR}$  column) in convective storms are indicative of a storm updraft. In addition, the launch of GOES-R will couple new tools that can be used to interrogate severe storms in real-time with increased spatial and temporal resolution. Combined, these remote sensing tools may eventually serve as nowcasting aids for forecasters in determining if severe weather is imminent. **While polarimetric radar data and new GOES-R products have been used to study severe storms, the radar and satellite products have not yet been compared with each other during a storm life cycle.**

**Past work:** A number of studies have shown that radar-observed  $Z_{DR}$  columns are formed from the lofting of rain and hail by a storm's updraft and act as a storm updraft proxy. Recent modeling work has established that  $Z_{DR}$  column characteristics can be used to gauge the strength of a storm updraft (Fig 1).

Separately, vigorous convection often results in cumulus cloud development through a storm's anvil, an overshooting top (OT). Many past studies have correlated the presence of a prolonged OT with the onset of severe weather soon after. In addition, the degree to which infrared window brightness temperatures (BT) cool (CTC) also can indicate enhanced vertical motion. Both OTs and CTC can be observed in satellite data.

## Objective

Use polarimetric radar and satellite data to examine how multiple proxies for a storm updraft compare to each other during the life cycle of a tornadic supercell thunderstorm. **The focus of this work is on: the relationship between  $Z_{DR}$  column height and CTC values, how  $Z_{DR}$  column heights change when OTs are detected, and how trends in the  $Z_{DR}$  column height and OT products compare during the tornado life cycle.**

## Data and Methods

- Radar:
  - KFDR data were analyzed from 1900–2300 UTC on 19 May 2015 for a twice tornadic supercell (see below for storm details).
  - A novel  $Z_{DR}$  column algorithm (Snyder et al. 2015) was run on the KFDR data. The algorithm provides the approximate altitude above mean sea level of the top of the 1 dB  $Z_{DR}$  column.
- Satellite:
  - Data from GOES-14 run in Super Rapid Scan Operations for GOES-R (SRSOR) mode were analyzed. SRSOR mode is meant to mimic the increased temporal resolution of GOES-R with 1-min updates. 1-min data from 1900–2300 UTC were analyzed.
  - The UW–CTC algorithm (Sieglaff et al. 2014) and GOES-R OT (Bedka et al. 2012) algorithms were used in this study. For the former, a 15-min running normalized difference of BT was used, and for the latter, the binary OT and OT magnitude products were investigated.

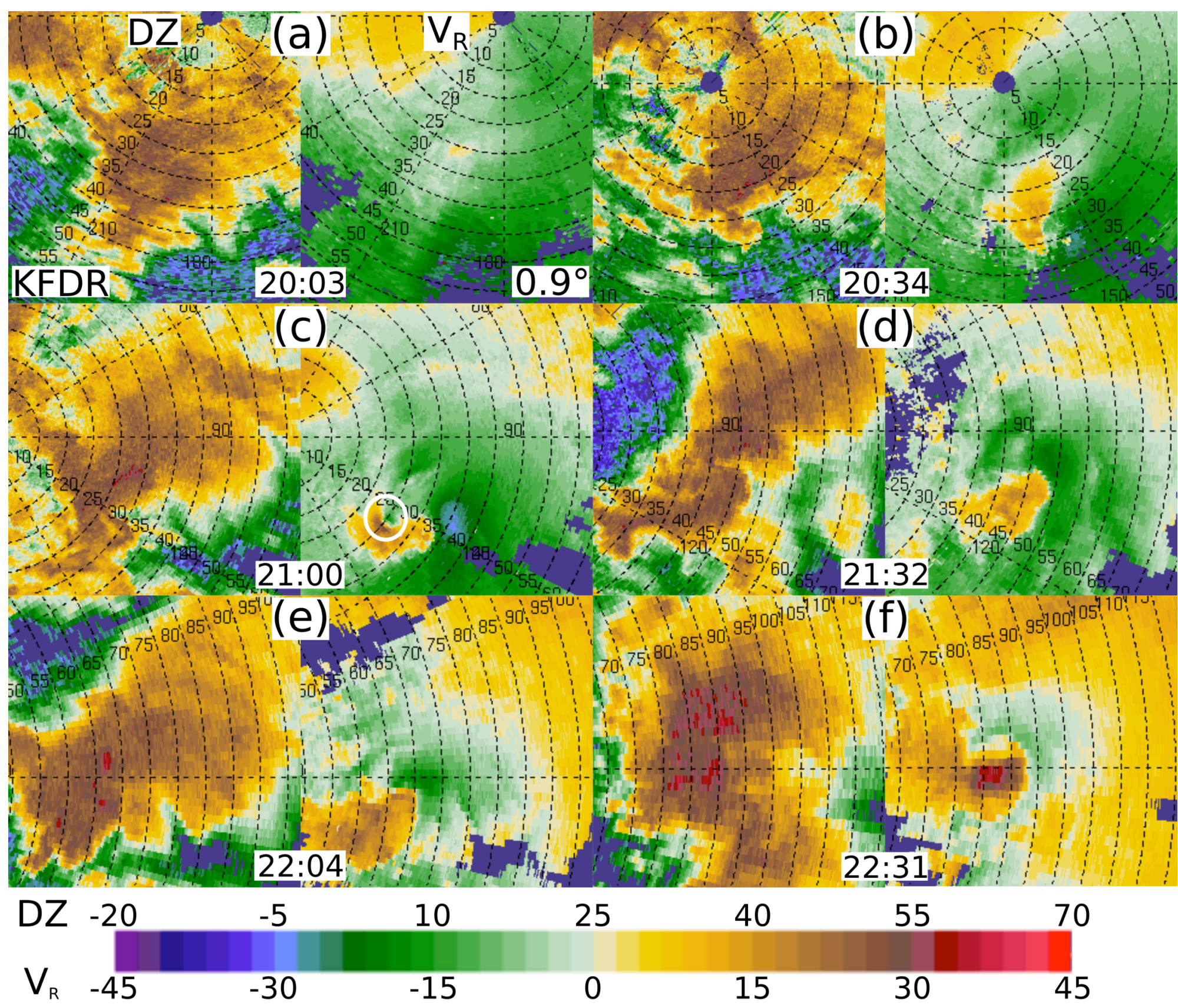


**Figure 2.** PPIs of reflectivity (left) and radial velocity ( $m s^{-1}$ ; right) at (a) 2003, (b) 2034, (c) 2100, (d) 2132, (e) 2204, and (f) 2231 UTC. The white circle in (c) marks the tornadic vortex signature associated with the second tornado. Range rings are every 5 km. Approximate center-beam heights vary from ~300-1300 m ARL. Up is due north.

**$Z_{DR}$  column height vs. CTC values:** The maximum  $Z_{DR}$  column height associated with the Red River supercell was extracted for each volume scan from 1900-2000 UTC and then compared with the CTC values (Fig. 3) from 1915-2000 UTC to examine their relationship during the storm's formation and early intensification phase.  $Z_{DR}$  column height steadily increased from 1900-1930 before leveling off. **During the times the CTC algorithm was able to return a value, it returned cooling rates that trended similarly to the  $Z_{DR}$  column height.** At the times when both column heights and CTC values were available within 1-min of each other, there was a tendency for higher heights to be associated with greater cooling rates, though the sample size is far too low for rigorous analysis. Based on past work (e.g., Fig. 1), the greater cooling rates and increased column heights were likely associated with enhanced vertical motion in the developing supercell.

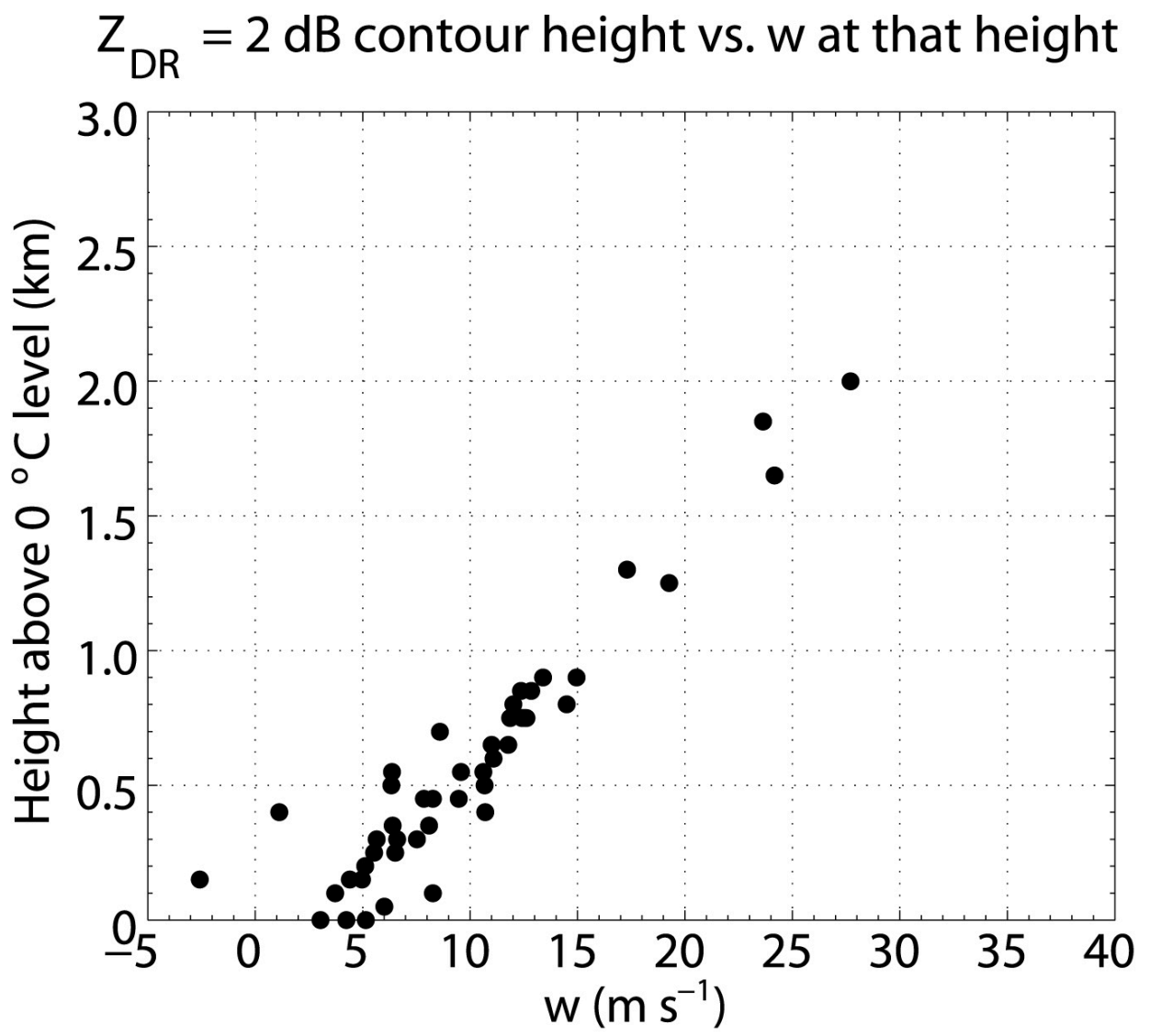


**Figure 1.** Scatterplot showing the relation between 2-dB  $Z_{DR}$  contour height above the  $0^{\circ}C$  level (km) and the updraft speed ( $m s^{-1}$ ) at that height. From Kumjian et al. (2014).

## Observations

### 19 May 2015 Red River Supercell:

The storm in question formed in NW Texas prior to 1900 UTC on 19 May 2015 (not shown). By 2000 UTC, it began to take on supercell characteristics (Fig. 2a). Shortly thereafter, a brief EF0 tornado was estimated to have formed at 2033 UTC in Wichita County, TX, just S of the Red River (Fig. 2b). A second tornado was observed by several spotters at ~2054 UTC in Tillman County, OK, NE of the Red River (Fig. 2c). This second tornado was larger and lasted for ~10 min.; it also was rated EF0 owing to a lack of observed damage. Following the dissipation of the second tornado, the storm took on the appearance of an HP supercell (Fig. 2d,e) before it interacted with another supercell to its south (Fig. 2f) and then evolved into a convective line segment after 2300 UTC (not shown).

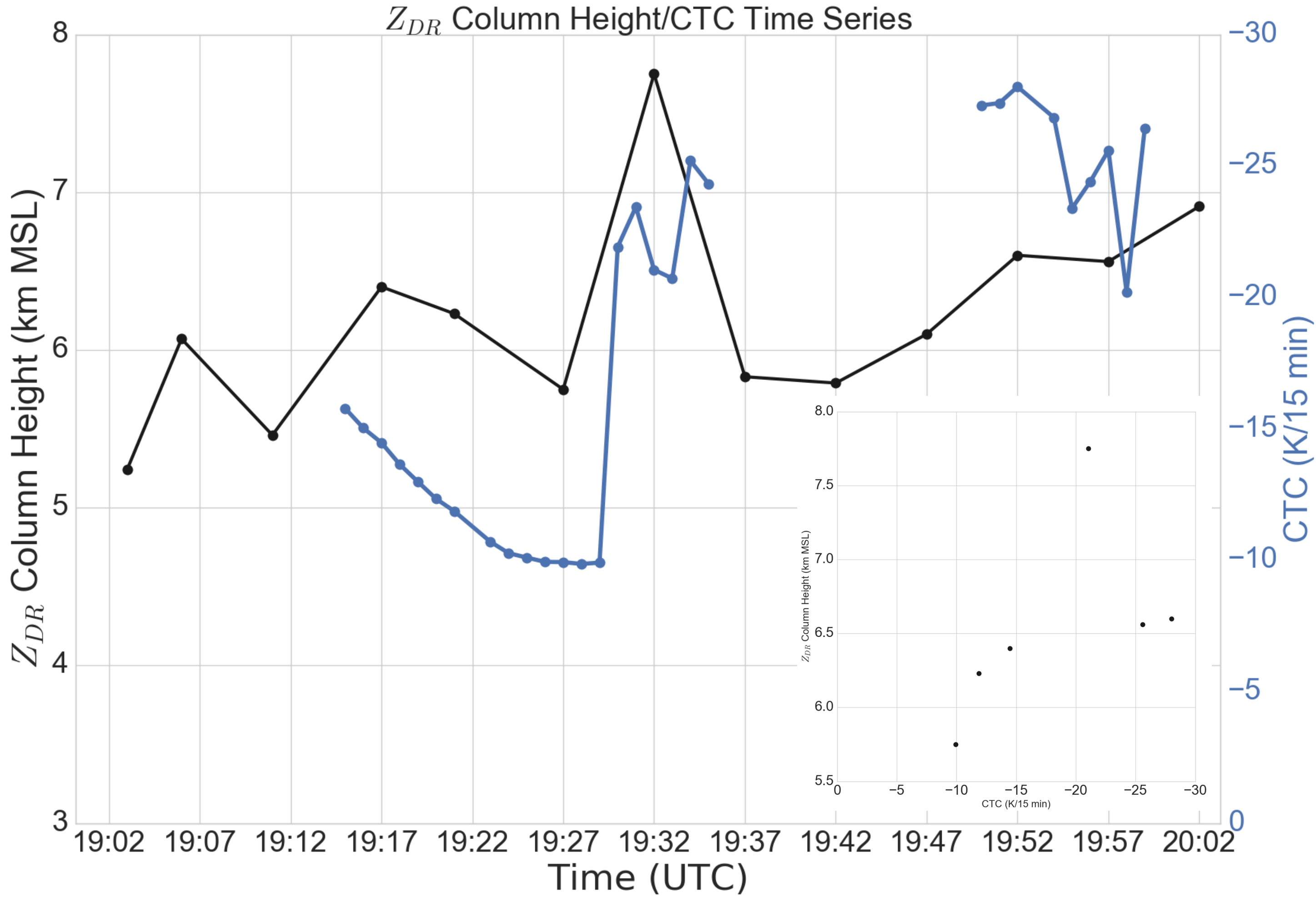


**Figure 3.** Time series of  $Z_{DR}$  column height (km above MSL; black) and CTC ( $K/15 min$ ; blue) from ~1900-2000 UTC during the period the Red River supercell was intensifying and transitioning to a supercell. (inset) Scatterplot of  $Z_{DR}$  column height vs. CTC at the times when both the relevant radar and satellite data were available.

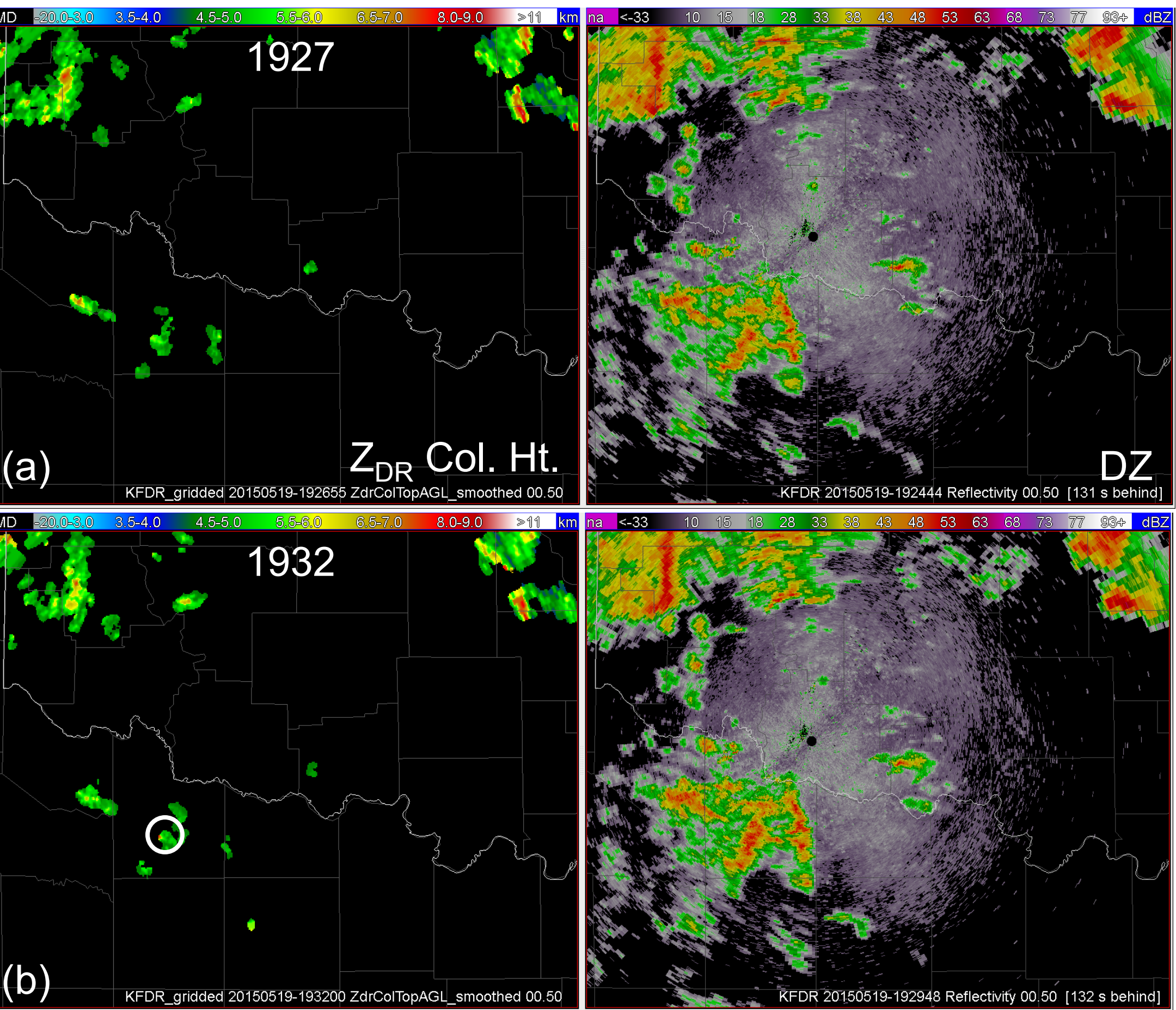
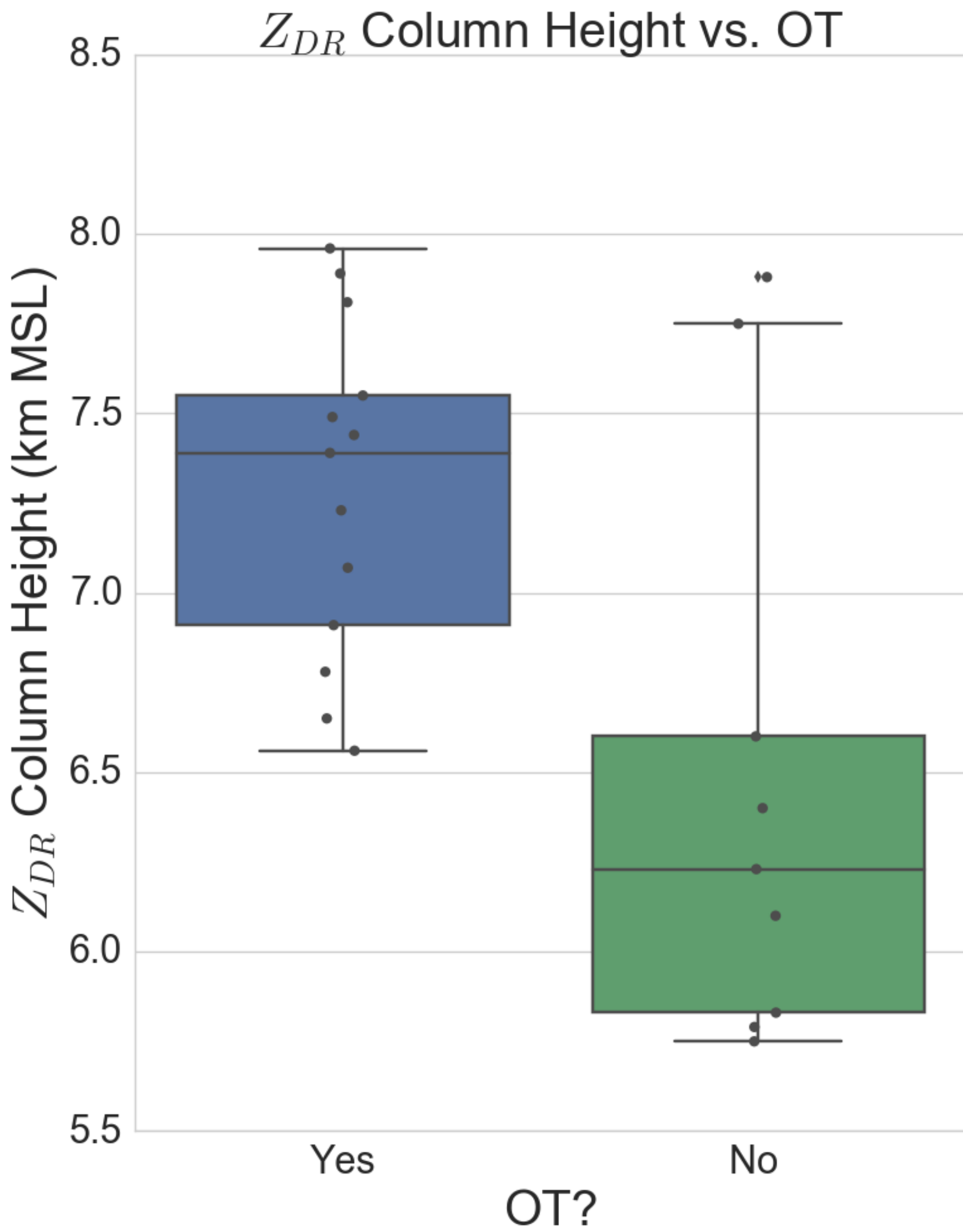


**Figure 4.** (left) Gridded  $Z_{DR}$  column height (km MSL) and (right) radar reflectivity (dBZ) at (a) 1927 and (b) 1932 UTC on 19 May 2015. The area of enhanced  $Z_{DR}$  column height associated with the developing Red River supercell is outlined by a white circle in (b).

**Figure 5.** Boxplots of  $Z_{DR}$  column heights (km MSL) for radar volumes in which an OT was (blue) and was not (green) detected. The raw data points are overlaid as gray circles. The diamond indicates an outlier value. A radar volume was associated with an OT detection if one occurred within 2 min of the radar analysis time.

### $Z_{DR}$ column heights and OTs:

The same methods were applied to comparisons between the  $Z_{DR}$  column heights and values from the OT algorithm. From the period 1915-2105 UTC (storm intensification through second tornado life cycle), satellite data were interrogated to determine if there was an OT "hit" associated with the Red River supercell. The  $Z_{DR}$  column heights of volumes that included an OT hit were compared with those that did not (Fig. 5).  **$Z_{DR}$  column heights were consistently higher when an OT was detected;** higher heights occurred at later time periods when the storm began to take on supercellular characteristics and when two tornadoes were reported.



### $Z_{DR}$ column height vs. CTC values, continued:

One potentially useful aspect of these tools is displayed in Fig. 4. As shown in Fig. 3, there is a noticeable jump in both  $Z_{DR}$  column height and in the amount of CTC between 1927 and 1932 UTC. In the following minutes, the storm enlarged greatly in size and took on supercell characteristics (Fig. 2a). The likely increase in vertical motion that contributed to these values could not be observed in radar reflectivity (Fig. 4) or in the radial velocity field (e.g., Fig. 2a). Also, the increased sampling in time allows GOES-14 in SRSOR mode to pick up the enhancement 3-min prior to KFDR.

**$Z_{DR}$  column height vs. OT magnitude:** For the times that an OT was detected in GOES-14 data, the OT magnitude, which measures how much colder the OT is than the adjacent anvil in K, also was interrogated. An ~1 hour time series shows the  $Z_{DR}$  column heights and OT magnitudes during the mature stage of the supercell, including during both tornadoes (Fig. 6).  **$Z_{DR}$  column height generally increased and OT magnitude consistently decreased during this time period.** This result complicates any attempt to establish a formal relationship between OT and  $Z_{DR}$  column height from this one case.

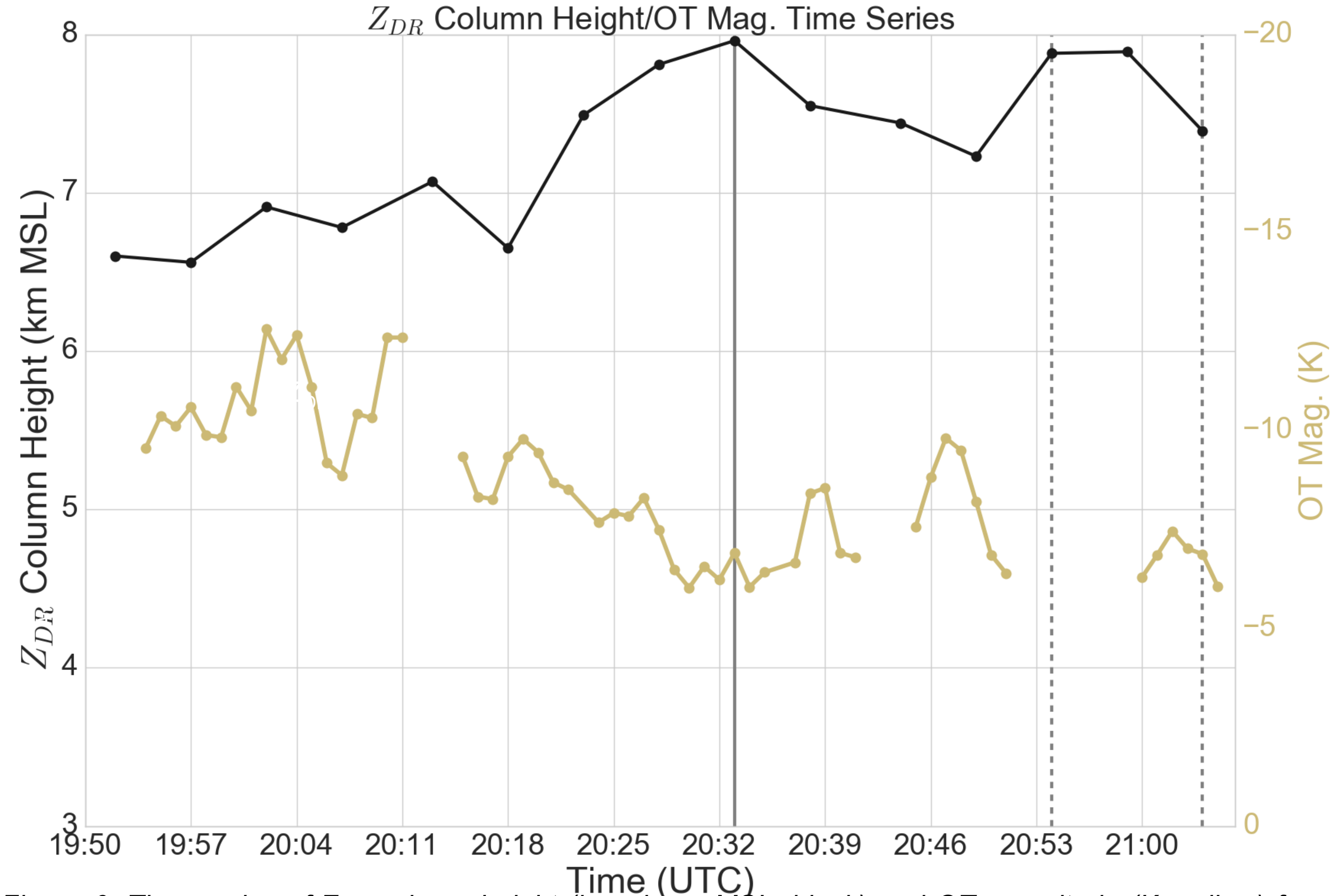


**Figure 6.** Time series of  $Z_{DR}$  column height (km above MSL; black) and OT magnitude (K; yellow) from ~1950-2105 UTC during the period the Red River supercell was mature and tornadic. The formation/dissipation time of the first tornado is shown by a straight gray line and the life cycle of the second tornado is enclosed by the gray dotted lines. Tornado begin/end times are estimates from Storm Data.

**Algorithm comparison during tornado life cycles:** Prior to both tornadoes, the maximum  $Z_{DR}$  column height increased and the magnitude of the OT temperature difference with the surrounding anvil decreased. Previous studies have not established a link between  $Z_{DR}$  column heights and tornado life cycles, however there are several previous observations of OT "collapse" prior to tornado formation. One downside of using a point value to represent  $Z_{DR}$  column height is that the general structure and areal values associated with the column are neglected. In the case of the second tornado, the general size, shape, and height values within the column remain similar, though the max. height value does increase, prior to and through its life cycle (Fig. 7).

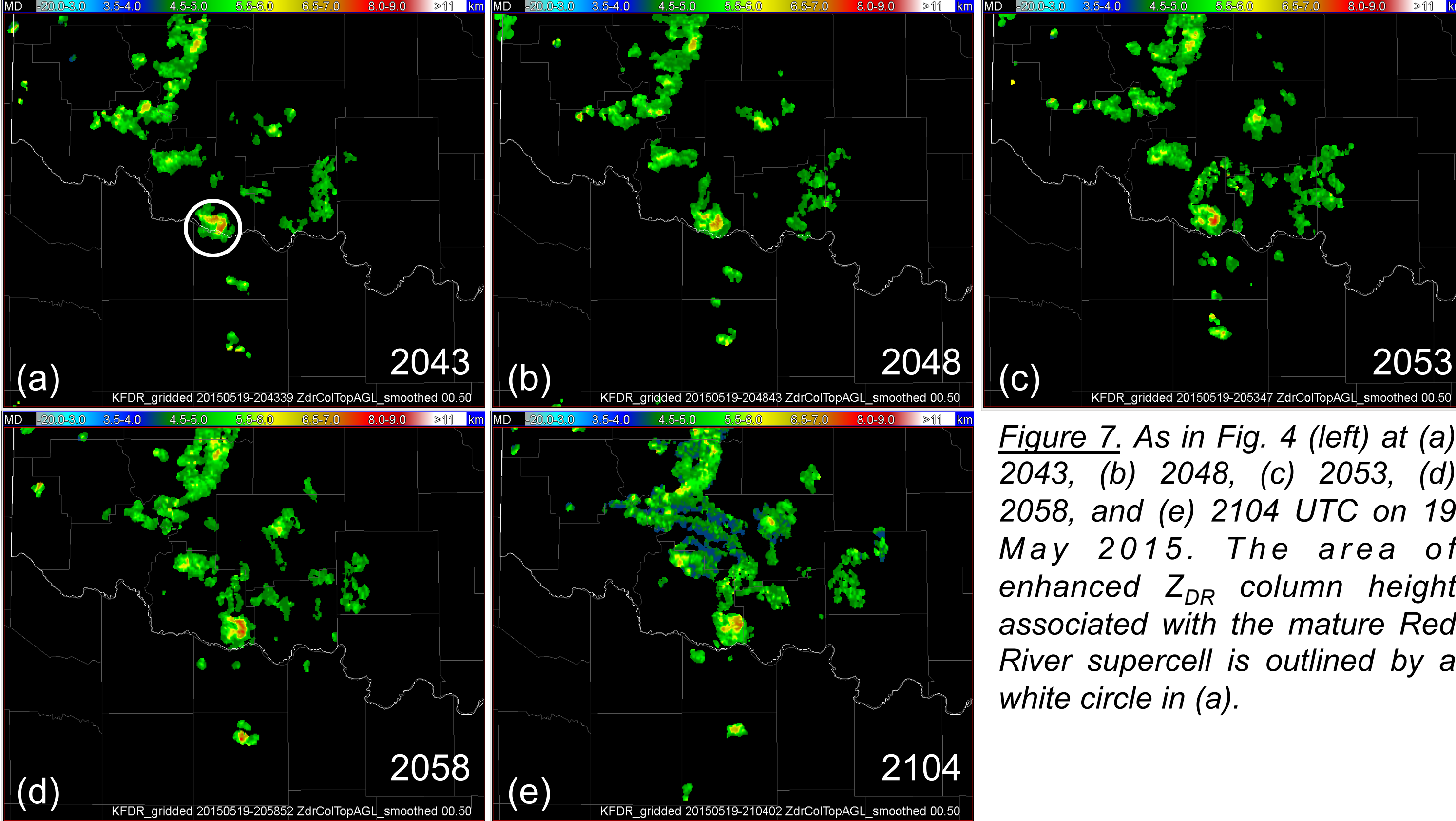


**Figure 7.** As in Fig. 4 (left) at (a) 2043, (b) 2048, (c) 2053, (d) 2058, and (e) 2104 UTC on 19 May 2015. The area of enhanced  $Z_{DR}$  column height associated with the mature Red River supercell is outlined by a white circle in (a).

## Future Work

Much additional work is necessary before any conclusions can be drawn about the relationship between radar and satellite products that are thought to act as proxies for a storm updraft or may indicate changes in updraft strength:

- More SRSOR cases are needed** to increase the data sample in order to rigorously assess statistical relationships amongst the products.
- Incorporation of other observationally-based updraft proxies is planned**, including radar updraft products currently under development and the lightning jump product.
- Additional focus on storm processes beyond tornado formation/dissipation**, including storm intensification, which may exhibit more robust signals and offer more operational utility.
- Exploration of potential symbiotic relationships among various updraft products** that may enhance operational confidence that updraft strength is being correctly inferred.

**Acknowledgments:** This work was supported by NASA grant NNX15AQ59G. The second author was supported with funding provided by NOAA/Office of Oceanic and Atmospheric Research under NOAA-University of Oklahoma Cooperative Agreement #NA11OAR4320072, U.S. Department of Commerce. The statements, findings, conclusions, and recommendations are those of the author(s) and do not necessarily reflect the views of NOAA or the U.S. Department of Commerce. The authors thank Kristin Calhoun, John Cintineo, and Lee Counce for helpful discussions and/or SRSOR data processing.